

Transport properties of Pb-doped $\text{Bi}_{4-n}\text{Pb}_n\text{Sr}_3\text{Ca}_3\text{Cu}_4\text{O}_x$ semiconducting glasses and glass-ceramic superconductors

S. Chatterjee, S. Banerjee, S. Mollah, and B. K. Chaudhuri

Department of Solid State Physics, Materials Research Section, Indian Association for the Cultivation of Science, Calcutta-700 032, India

(Received 27 April 1995; revised manuscript received 7 August 1995)

Electrical conductivity and thermoelectric power (TEP) of the as-quenched and annealed (at 500 °C for 10 h and 840 °C for 24 h) $\text{Bi}_{4-n}\text{Pb}_n\text{Sr}_3\text{Ca}_3\text{Cu}_4\text{O}_x$ ($x = 0-1.0$) glasses have been measured. The dc conductivity data of the as-quenched and the partially annealed (at 500 °C) glasses can be explained by considering the small-polaron hopping conduction mechanism which is found to change from the nonadiabatic to the adiabatic regime with annealing the glasses at 500 °C. This change over is due to the presence of microcrystals in the partially annealed glasses as observed from x-ray-diffraction and scanning electron microscopic studies. This adiabatic behavior is also visualized even for some as-quenched glasses having a very small amount of the more conducting microcrystalline phase. All the 840 °C annealed glasses are superconductors with T_c between 110 and 115 K. The Seebeck coefficient (S) of the partially annealed glass system is found to be positive and increases linearly with temperature. The S values of the corresponding glass-ceramic superconductors showing broad peaks around T_c . A change over in the values of S from positive (below ~ 290 K) to negative (above ~ 290 K) indicates the coexistence of both electrons and holes in these superconductors. The TEP data can be fitted with both the two-band model of Forro *et al.* [Solid State Commun. **73**, 501 (1990)] and the Nagaosa-Lee model [Phys. Rev. Lett. **64**, 2450 (1990)]. Therefore, the bosonic contribution in the transport properties of these superconductors, as suggested by the Nagaosa-Lee model, is supported.

I. INTRODUCTION

The glassy precursors for high- T_c superconductors like $\text{Bi}_{4-n}\text{Pb}_n\text{Sr}_3\text{Ca}_3\text{Cu}_4\text{O}_x$ are very interesting because of several reasons. There is immense possibility of making superconducting wire/tapes, and thick films¹⁻³ for technological applications. Therefore, elaborate investigations of various physical properties of these special type of glassy and corresponding glass-ceramic (GC) phases are important. Among the possible coexisting phases in the Bi-Sr-Ca-Cu-O systems,^{4,5} the 80 K phase forms more easily. This phase is also thermodynamically more stable. Partial substitution of Bi by Pb enhances the preparation of the nearly single phase (2223) superconductor ($T_c \sim 110$ K).^{6,7} Endo *et al.*⁸ proposed that Pb^{+2} substituted for Bi^{+3} as well as Sr defects act as hole donors. Since the valency of Pb is +2 and that of Bi is +3, one Pb atom can dope a hole to the system. Study of thermoelectric power of this system would be important to find the nature of the carriers (holes or electrons). As the Pb-doped (2223) phase has the high- T_c value (~ 115 K), it is interesting to process this phase via controlled crystallization of the corresponding glassy precursor phase.

Recently, several investigations of the superconducting behavior of the Pb-doped Bi-Sr-Ca-Cu-O system have been made.^{9,10} But the comparative study of the semiconducting properties of the as-quenched and the corresponding partially annealed (with the appearance of micro crystals) glassy systems have not been made so far. Here it is interesting to point out that the appearance of microcrystals (more conducting crystalline phases) in the as-quenched glass (by partial annealing or produced during glass formation) changes the hopping conduction mechanism (nonadiabatic to adiabatic) along with other behavior. Furthermore, very little or no re-

port has been made so far on the detailed thermoelectric powers of these glassy precursors and those of the corresponding glass-ceramic (GC) superconductors,

The purpose of the present paper is to study the effect of annealing time and temperature on the electrical conductivity and thermoelectric power (TEP) of the $\text{Bi}_{4-n}\text{Pb}_n\text{Sr}_3\text{Ca}_3\text{Cu}_4\text{O}_x$ ($0.1 \leq n \leq 1.0$) glasses which are very good precursors of high- T_c superconductors. The $\text{Bi}_4\text{Sr}_3\text{Ca}_3\text{Cu}_4\text{O}_x$ or (4334) system has been chosen as the mother glassy phase because it is easily converted¹¹ to single phase $\text{Bi}_2\text{Sr}_2\text{Ca}_1\text{Cu}_2\text{O}_y$ or [2212] superconductor. Furthermore, transport properties of Li-doped $\text{Bi}_4\text{Sr}_3\text{Ca}_3\text{Cu}_4\text{O}_x$ glassy system have also been elaborately studied earlier^{12,13} using small polaron hopping conduction mechanism. However, there is still a controversy over the true mechanism (adiabatic or nonadiabatic) of conduction in the glassy precursors of high- T_c superconductors. While the nonadiabatic small polaron hopping conduction mechanism is found to be valid for the Li-doped (4334) glasses.¹² Singh and Zacharias¹⁴ argued that the polaron hopping mechanism is in the adiabatic regime in such glassy semiconductors. Therefore, the semiconducting behavior of the as-quenched Pb-doped $\text{Bi}_4\text{Sr}_3\text{Ca}_3\text{Cu}_4\text{O}_x$ (4334) glasses, behaving similarly to those of the corresponding Li-doped glasses,^{12,15} has also been studied. From the present investigation, it would be visualized how the model parameters like Debye temperature, phonon frequency, conduction mechanism (nonadiabatic to adiabatic) and microstructure change in the Pb-doped (4334) glasses due to annealing.

Since the theoretical analysis of the experimental dc conductivity of the as-quenched Pb-doped (4334) glasses can be made similarly to that of the Li-doped (4334) glasses¹² (hereafter referred to as Ref. 1), we shall only briefly discuss the

results on dc conductivity data of the present as-quenched glasses for comparison with those of the partially annealed semiconducting glasses.

In Sec. II sample preparation and different techniques used have been discussed in short. Section III deals with the microstructural properties of the glasses and glass ceramics. Analysis of the dc conductivity data of the as-quenched, partially annealed glasses and the corresponding superconducting glass ceramics have also been made in this section. The thermoelectric power data of the glassy semiconductors and the corresponding glass-ceramic superconductors have been discussed in Sec. IV. The paper ends with a brief summary and conclusion in Sec. V.

II. EXPERIMENT

The $\text{Bi}_{4-n}\text{Pb}_n\text{Sr}_3\text{Ca}_3\text{Cu}_4\text{O}_x$ ($n=0.1, 0.5, 1.0$) glasses are prepared by rapid quenching technique discussed earlier¹⁵⁻¹⁷ and the glass samples thus prepared are divided into two batches. The first batch of the samples are annealed at 500 °C for 10 h. These samples are denoted by Pb1A, Pb2A, and Pb3A for $n=0.1, 0.5,$ and 1.0 , respectively. The second batch of the samples are heated at 840 °C for 24 h and then furnace cooled. These samples are termed as Pb1S, Pb2S, and Pb3S for $n=0.1, 0.5,$ and 1.0 , respectively. On annealing at these two temperatures in air, these glassy samples become partially (PbA-type) and completely (PbS-type) oxygenated and crystalline (also called glass ceramics). The total copper ion concentrations of the samples were determined from atomic absorption and the values of Cu^{2+} concentration were determined by chemical analysis as discussed earlier [Ref. 1]. The glass transition temperature (T_g) determined by thermal analysis and the results of infrared (IR) spectra showing the presence of BiO_3 and BiO_6 pyramidal and octahedral units have already been reported.¹⁶ Some important parameters of the glasses are shown in Table I for comparison.

Both the as-quenched and the annealed systems are characterized by x-ray powder diffraction (Philips, Model PW 1710) and scanning electron micrographs (Model 425A), Hitachi, Japan). The dc conductivity (σ_{dc}) and thermoelectric power (TEP) measurements were performed on all the samples with different Pb concentrations. The dc conductivity of the glassy samples was measured by two point method, whereas that of the conducting crystallized samples was measured by standard four probe technique using the APD cryocooler (Model: HC-2D) with helium refrigerating system and temperature controller. Conductivity measurements were made in the Ohmic region as tested from the study of the I-V curves. The dc conductivity of the same glass samples in different runs agreed within 2–3 % and samples of the same composition from different batches gave agreement within 5% for room temperature measurements. The temperature was measured with a nanovoltmeter (Keithley 181) with an accuracy of ± 0.5 K (or better). The TEP values of the glasses and glass-ceramic samples ($10 \times 4 \times 1 \text{ mm}^3$) were also measured with the use of the APD cryocooler and Keithley nanovoltmeter (Model 181). A temperature difference of 2–4 degrees was maintained between the two parallel surfaces of the samples under investigation.

TABLE I. Value of different parameters of the as-quenched $\text{Bi}_{4-n}\text{Pb}_n\text{Sr}_3\text{Ca}_3\text{Cu}_4\text{O}_x$ glasses.

Parameters	Pb1($n=0.1$)	Pb2 ($n=0.5$)	Pb3 ($n=1.0$)
T_g (°C) ^a	400±5	390±5	385±5
$C = \frac{\text{Cu}^{1+}}{\text{Cu}_{\text{tot}}}$	0.78	0.78	0.78
Density (gm/cc)	7.001	6.901	6.760
N (10^{19} cm^{-3})	2.72	0.63	4.00
R (Å)	4.61	4.69	4.72
r_p (Å)	1.88	1.89	1.90
θ_D (K)	420	412	408
ν_{ph} (10^{12} Hz)	8.75	8.58	8.50
$N(E_F)$ ($10^{21} \text{ eV}^{-1} \text{ cm}^{-3}$)	9.75	9.64	9.47
α (Å ⁻¹) ^b	0.341	0.384	0.383
α (Å ⁻¹) ^c	0.407	0.250	0.464
W (eV) (at 300 K)	0.512	0.580	0.443
W_H (eV)	0.295	0.296	0.295
γ	14.261	14.342	14.258

^aObtained from the differential thermal analysis (DTA).

^bObtained from Eq. (1).

^cObtained from Greaves' model [Eq. (4)].

III. RESULTS AND DISCUSSIONS

A. Structural properties of the glasses and glass ceramics

The XRD patterns of the as-quenched glasses shown in Fig. 1 indicate glassy behavior. Figure 2 shows the XRD patterns of the partially annealed (500 °C for 10 h) Pb1A, Pb2A, and Pb3A samples and the corresponding XRD patterns of the Pb1S, Pb2S, and Pb3S glass ceramics (annealed at 840 °C for 24 h) are shown in Fig. 3. The appearance of sharp peaks in Fig. 3 is due to the formation of crystalline phases. The identified crystalline peaks in the partially annealed samples (Fig. 2) are found to be of Cu_2O , Ca_2PbO_4 , Bi_2O_3 , PbO , and Bi-2201 , Bi-2212 , Bi-

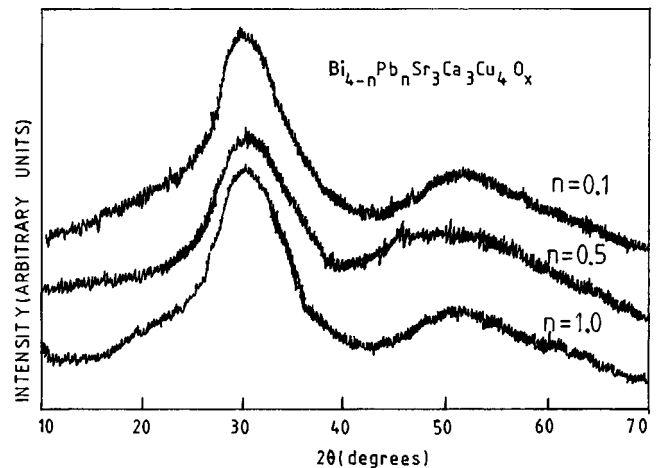


FIG. 1. X-ray-diffraction pattern of $\text{Bi}_{4-n}\text{Pb}_n\text{Sr}_3\text{Ca}_3\text{Cu}_4\text{O}_x$ as-quenched glasses: (a) $n=0.1$, (b) $n=0.5$, and (c) $n=1.0$.

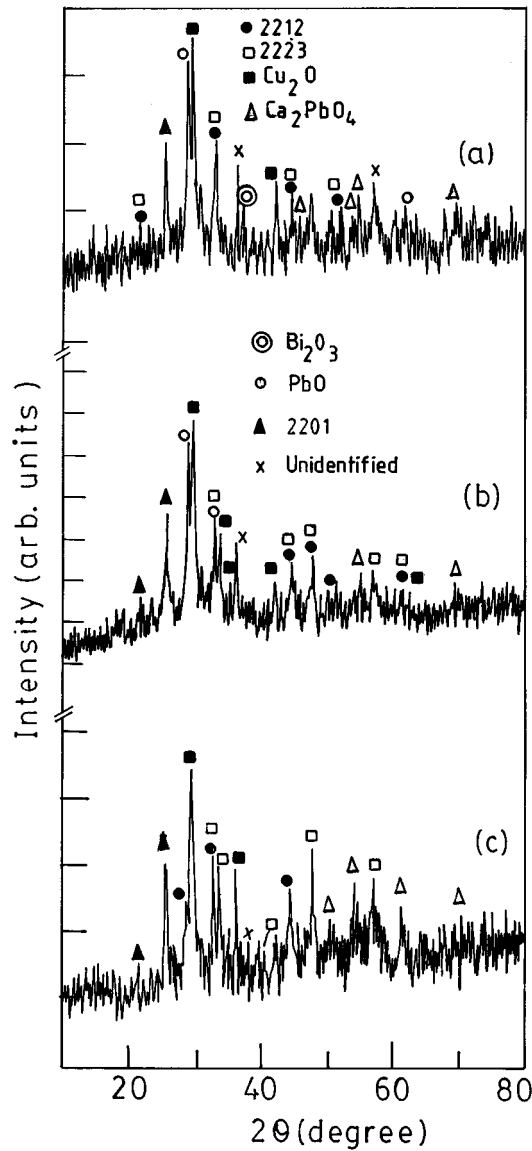


FIG. 2. X-ray-diffraction pattern of $\text{Bi}_{4-n}\text{Pb}_n\text{Sr}_3\text{Ca}_3\text{Cu}_4\text{O}_x$ glass ceramics annealed at 500°C for 10 h: (a) Pb1A ($n=0.1$), (b) Pb2A ($n=0.2$), and (c) Pb3A ($n=1.0$).

2223 phases. There are also some unidentified peaks (indicated by cross marks) in Fig. 2. However, after final heating at 840°C (for 24 h) the samples become superconductors having mostly superconducting 2212 and 2223 phases along with traces of Ca_2PbO_4 phase. At this annealing temperature the additional phases formed in the samples during the partial heating at 500°C disappear. Similar crystallization kinetics of this type of glasses was also discussed in a recent review by Bansal.¹⁸ The XRD pattern of the glass-ceramic samples (Fig. 3) annealed at 840°C for 24 h (which are superconducting as discussed below) can be fitted with the pseudotetragonal structure. The lattice parameters thus obtained for the Pb1S, Pb2S, and Pb3S superconducting samples are given in Table II. These values of the lattice constants agree quite well with the reported values¹⁹ of the corresponding superconducting samples.

The scanning electron micrographs (SEM) of a typical as-quenched glass sample (viz. $\text{Bi}_{3.5}\text{Pb}_{0.5}\text{Sr}_3\text{Ca}_3\text{Cu}_4\text{O}_x$) and the corresponding glass ceramics are shown in Fig. 4.

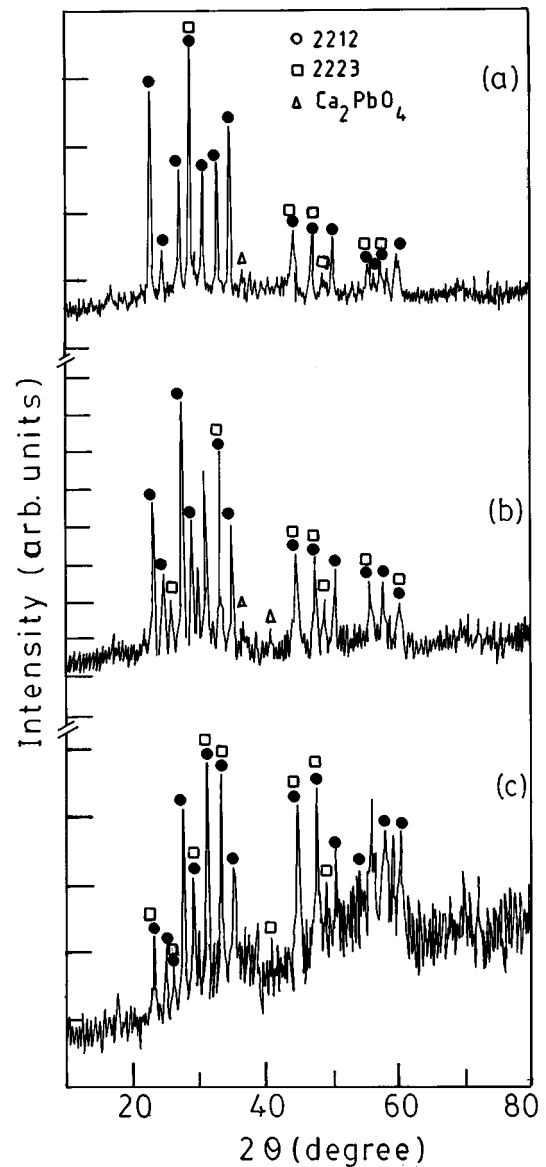
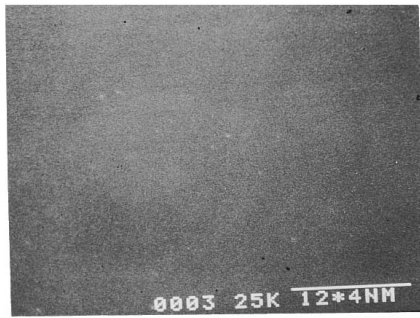


FIG. 3. X-ray-diffraction pattern of $\text{Bi}_{4-n}\text{Pb}_n\text{Sr}_3\text{Ca}_3\text{Cu}_4\text{O}_x$ glass-ceramic superconductors (glasses annealed at 840°C for 24 h): (a) Pb1S ($n=0.1$), (b) Pb2S ($n=0.5$), and (c) Pb3S ($n=1.0$).

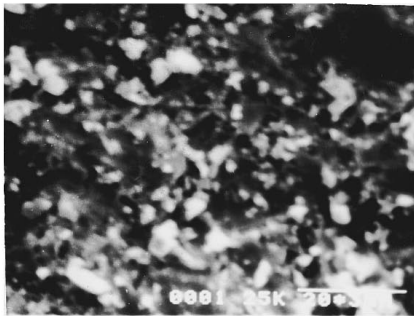
Other samples also show identical features. The glass samples annealed at 500°C for 10 h display [Fig. 4(b)] features of $3\text{--}10\ \mu\text{m}$ in size. The homogeneously distributed particulate feature of the crystallites seen in the samples annealed at 500°C is considered to arise from copious nucle-

TABLE II. Values of the lattice constants (fitted with tetragonal structure) and superconducting transition temperatures T_{c0} (zero resistance temperature) of superconducting glass ceramics (the $\text{Bi}_{4-n}\text{Pb}_n\text{Sr}_3\text{Ca}_3\text{Cu}_4\text{O}_x$ glasses annealed at 840°C for 24 h).

Superconducting glass ceramics	Lattice constants (\AA)				T_{c0} (K)
	2212 phase		2223 phase		
	a	c	a	c	
Pb1S	5.4142	30.7460	5.3247	37.7047	72
Pb2S	5.4067	30.7333	5.6455	37.0199	73
Pb3S	5.3949	30.5793	5.7127	37.5441	78



(a)



(b)



(c)

FIG. 4. Scanning electron micrographs of $\text{Bi}_{4-n}\text{Pb}_n\text{Sr}_3\text{Ca}_3\text{Cu}_4\text{O}_x$ (for $n=0.5$) as as-quenched glass (a), the glass-ceramic annealed at 500°C for 10 h (Pb2A) (b), and the superconducting glass-ceramic annealed at 840°C for 24 h (Pb2S) (c). [Scale: (a) 23 mm = $120\ \mu\text{m}$, (b) 20 mm = $20\ \mu\text{m}$, and (c) 20 mm = $10\ \mu\text{m}$.]

ation in the phase separated microstructures of the as-quenched glasses. The glass ceramics annealed at 840°C , however, show pure crystalline structure [Fig. 4(c)].

B. Electrical conductivities of as-quenched glasses

The thermal variation of σ_{dc} of the Pb-doped (4334) glasses are almost similar to those of the Li-doped (4334) glasses discussed earlier [Ref. 1]. Variation of dc conductivity (σ_{dc}) as a function of inverse temperature and $\sigma_{\text{dc}}T^{1/2}$ as a function of $T^{-1/4}$ are shown, respectively, in Figs. 5 and 6.

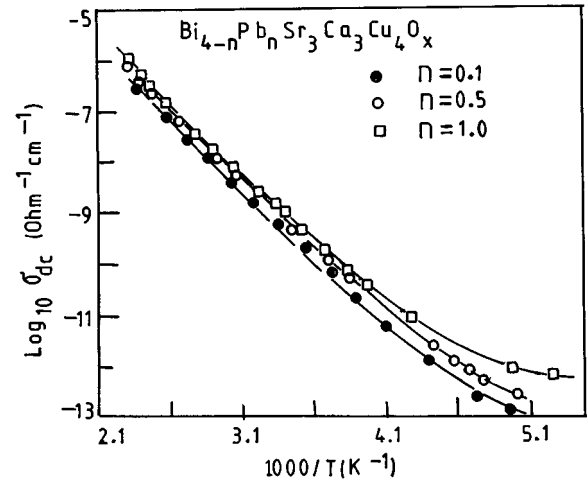


FIG. 5. The logarithm of dc conductivity of the as-quenched $\text{Bi}_{4-n}\text{Pb}_n\text{Sr}_3\text{Ca}_3\text{Cu}_4\text{O}_x$ (for $n=0.1, 0.5, 1.0$) glasses as a function of T^{-1} .

These data can be analyzed with nearest-neighbor hopping of small polarons, proposed by Mott^{20,21} (for the region of $T > \theta_D/2$, θ_D being the Debye temperature) and Greaves' variable range hopping²² (for $T < \theta_D/2$) as discussed below. The expression for the dc conductivity (σ_{dc}) as proposed by Mott^{20,21} can be written as (for $T > \theta_D/2$)

$$\sigma_{\text{dc}} = [\nu_{\text{ph}} N e^2 R^2 C (1 - C) \exp(-2R\alpha) \exp(-W/k_B T)] / k_B T, \quad (1)$$

where N , ν_{ph} , α^{-1} , R , W , and C , are, respectively, the number of transition metal (Cu) ion per unit volume, the optical phonon frequency, localization length of the s -like wave function assumed to describe the localized states at each transition metal (Cu) ion site, average intersite separation, activation energy for the hopping conduction and the ratio of the transition metal (TM) ion concentration in the low valence states to the total TM ion concentrations. In Eq. (1) k_B and T are Boltzmann constant and absolute temperature, respectively. Assuming a strong electron-phonon coupling²³ the activation energy W is given by

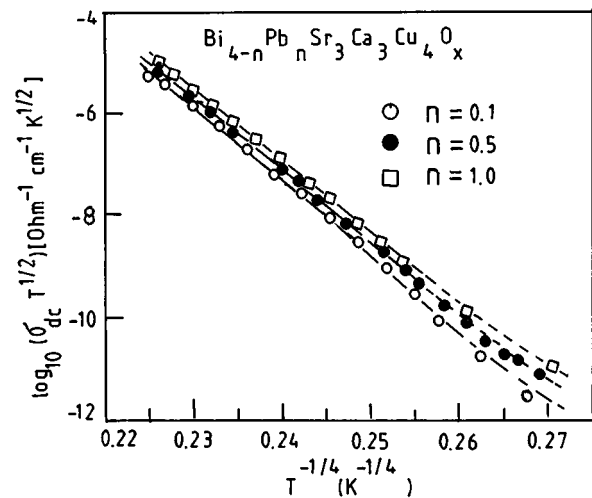


FIG. 6. The variation of $\log_{10}(\sigma_{\text{dc}} T^{1/2})$ with $T^{-1/4}$ of the as-quenched $\text{Bi}_{4-n}\text{Pb}_n\text{Sr}_3\text{Ca}_3\text{Cu}_4\text{O}_x$ glasses.

$$W = W_H + W_D/2 \quad (\text{for } T > \theta_D/2) = W_D \quad (\text{for } T < \theta_D/4), \quad (2)$$

where W_H and W_D are, respectively, the polaron hopping energy and disorder energy arising from the variation of local arrangements of the ions, and θ_D , defined by $h\nu_{\text{ph}} = k_B\theta_D$, is the characteristic Debye temperature. In the adiabatic limit, the overlap integral $I = \exp(-2\alpha R)$ in Eq. (1) reduces to unity.

Schnakenberg²⁴ also showed theoretically that in amorphous solids, for $T < \theta_D/2$ the contribution to σ_{dc} comes predominantly from acoustic phonon, while for $T > \theta_D/2$, the main contribution to σ_{dc} is the phonon assisted conductivity and hence the temperature dependence of conductivity is different in the temperature ranges on either side of $T_k \sim \theta_D/2$. Schnakenberg model predicts a sharp decrease in activation energy with decrease in temperature at T_k . The temperature dependent conductivity in this model has the form

$$\sigma_{\text{dc}} = \sigma_0 T^{-1} [\sinh(h\nu_{\text{ph}})]^{1/2} \exp[-(4W_H/h\nu_{\text{ph}}) \times \tanh(h\nu_{\text{ph}}\beta/4)] \exp(-W_D\beta), \quad (3)$$

where σ_0 is a temperature independent parameter and $\beta = 1/k_B T$.

The experimental conductivity data above a typical characteristic temperature T_k (say) ~ 250 K (where nonlinearity is observed in Fig. 5) are fitted with Eq. (1). The experimental conductivity data are fitted by least squares method similar to our earlier work [Ref. 1] and the best fit parameters are shown in Table I. The phonon frequency ν_{ph} are obtained from the infrared data.²⁵ The value of C is estimated from magnetic susceptibility and atomic absorption [Ref. 1]. The values of α shown in Table I are reasonable for localized states and indicate strong localization as in the case of Li-doped (4334) glasses and many other transition metal oxide (TMO) glasses as discussed in Ref. 1. An estimation of polaron radius r_p which is related²⁶ to W_H ($W_H = 4e^2/\epsilon_p r_p$) has also been made for all the glasses and are shown in Table I. The effective dielectric constant ϵ_p is obtained from dielectric constant data.^{15,16} The estimated values of r_p (as shown in Table I) also suggest that the polarons are highly localized in the undoped and Pb-doped $\text{Bi}_4\text{Sr}_3\text{Ca}_3\text{Cu}_4\text{O}_x$ glasses.

At sufficiently low temperatures where the polaron binding energy is small and static disorder energy of the glass plays a dominant role in the conduction process, Mott's $T^{-1/4}$ analysis for the variable range hopping (VRH) can, in general, be applied for the TMO glasses. But for the Pb-doped glasses, sufficient data at low temperature is not available due to experimental limitations and very high resistivity of the samples which is also found to be true for Li-doped $\text{Bi}_4\text{Sr}_3\text{Ca}_3\text{Cu}_4\text{O}_x$ glasses [Ref. 1]. An attempt to verify the applicability of this law gives unacceptably large values of α and W_D .

At the intermediate temperature region Greaves²² suggested a variable range hopping conduction and derived an expression for the conductivity as

$$\sigma_{\text{dc}} T^{1/2} = A \exp(-B/T^{1/4}), \quad (4)$$

where A and B are constants and $B = 2.1[\alpha^3/k_B N(E_F)]^{1/4}$, $N(E_F)$ is the density of states at the Fermi level. $N(E_F)$

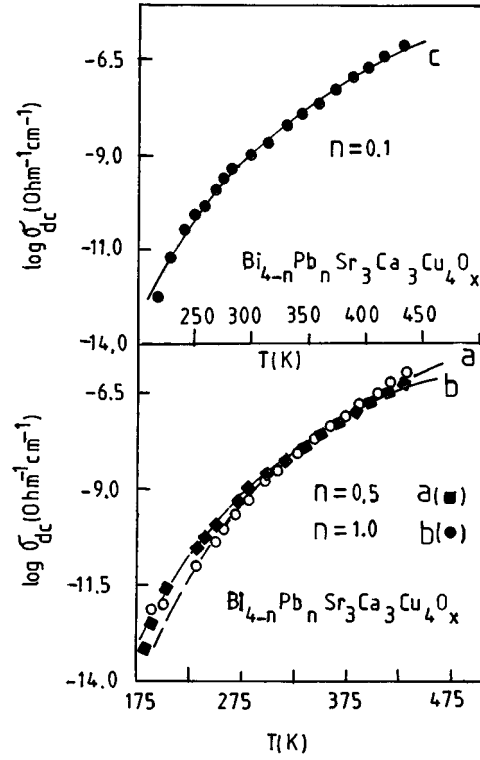


FIG. 7. Theoretical fitting of the dc-conductivity data with Eq. (3) of the as-quenched $\text{Bi}_{4-n}\text{Pb}_n\text{Sr}_3\text{Ca}_3\text{Cu}_4\text{O}_x$ glasses: (a) $n=0.5$, (b) $n=1.0$, and (c) $n=0.1$.

values (shown in Table I) are obtained from the ac conductivity data of these glasses.^{15,25} In Fig. 6 (continuous line), the experimental conductivity data in the low temperature region are fitted with Greaves' VRH model [Eq. (4)]. The values of α estimated from the best fit are also reasonable for localized states²⁷ and are consistent with the values obtained by the fitting of the conductivity data with Eq. (1) (as shown in Table I). Similar values of α are also obtained for the Li-doped $\text{Bi}_4\text{Sr}_3\text{Ca}_3\text{Cu}_4\text{O}_x$ glasses and other TMO glasses.^{12,15}

The experimental data has also been fitted with Schnakenberg model [Eq. (3)] as shown in Fig. 7. The best fit parameters are shown in Table III. W_H is almost same for all the as-quenched glasses, but it is different from the values obtained by the fitting with Mott's model (Table I). The values of W_D decreases with increase of Pb concentration in the (4334) glasses.

The hopping mechanism (adiabatic or nonadiabatic) of these glasses could be suggested²⁸ by plotting $\log_{10}(\sigma_{\text{dc}})$ vs W at a fixed temperatures. The temperature T_e (say), esti-

TABLE III. Best fit parameters obtained from Schnakenberg's conductivity equation [Eq. (3)] for the as-quenched $\text{Bi}_{4-n}\text{Pb}_n\text{Sr}_3\text{Ca}_3\text{Cu}_4\text{O}_x$ glasses with $n=0.1$ (Pb1), $n=0.5$ (Pb2), and $n=1.0$ (Pb3).

Glasses	ν_{ph} (Hz)	W_H (eV)	W_D (eV)
Pb1	2.0×10^{12}	0.468	0.050
Pb2	3.9×10^{12}	0.513	0.012
Pb3	5.2×10^{12}	0.513	0.009

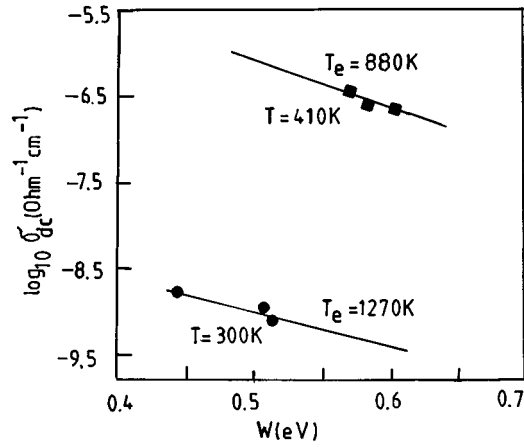


FIG. 8. The logarithm of dc conductivity of the as-quenched glasses as a function of W (activation energy), obtained from Fig. 5, at two fixed temperatures (300 and 410 K). The estimated temperature from slopes of these two curves are 1270 and 880 K, respectively.

mated from the slope of such a plot would be close to the experimental temperature when the hopping is considered to be in adiabatic regime. On the other hand, T_e would be very different from experimental temperature if the hopping is considered to be in the nonadiabatic regime. Such a plot for two fixed temperature ($T=300$ and 410 K) is shown in Fig. 8 and the corresponding T_e values estimated (1270 and 883 K, respectively) are very much different from experimental temperatures in the Pb-doped (4334) glasses. Thus the hopping mechanism of these as-quenched glasses is in the nonadiabatic regime as in the case of Li-doped $\text{Bi}_4\text{Sr}_3\text{Ca}_3\text{Cu}_4\text{O}_x$ glasses.^{12,15} The nonadiabatic hopping is also supported from the validity of Emil-Holstein relation.²⁹ According to this relation the polaron bandwidth J satisfies the inequality

$$J \gtrless (2k_B T W_H / \pi)^{1/4} (h\nu_{\text{ph}} / \pi)^{1/2}, \quad (5)$$

where the signs $>$ and $<$ are for adiabatic and nonadiabatic hopping, respectively. The values of $(2k_B T W_H / \pi)^{1/4} (h\nu_{\text{ph}} / \pi)^{1/2}$ vary from 0.0279 to 0.0284 at 300 K for all the concentrations. The values of J estimated independently from $J \approx \hbar e^3 [N(E_F) / \epsilon_p^3]^{1/2}$, are of the order of 0.022 eV. Thus, in Pb-doped glasses $J \ll (2k_B T W_H / \pi)^{1/4} (h\nu_{\text{ph}} / \pi)^{1/2}$ which suggests that the nearest-neighbor hopping mechanism occurs in the nonadiabatic regime. This behavior is also similar to the Li-doped $\text{Bi}_4\text{Sr}_3\text{Ca}_3\text{Cu}_4\text{O}_x$ glasses reported earlier [Ref. 1].

C. Electrical conductivity of partially annealed glasses and glass-ceramic superconductors

The dc conductivity data of the corresponding partially annealed (annealed at 500°C for 10 h) $\text{Bi}_{4-n}\text{Pb}_n\text{Sr}_3\text{Ca}_3\text{Cu}_4\text{O}_x$ ($n=0.1, 0.5, 1.0$) glasses also showing semiconducting behavior (Fig. 9) can also be similarly analyzed by using the polaron hopping conduction mechanism. However, in this case, as discussed below, the nature of the polaron hopping conduction mechanism changes from nonadiabatic regime to adiabatic regime.

The semiconducting character of these samples is clearly observed from the temperature dependence of conductivity

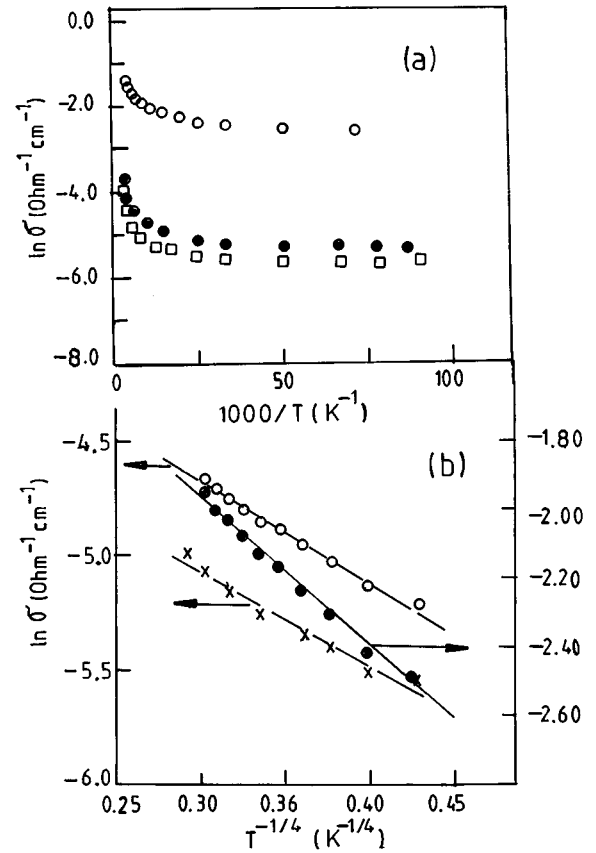


FIG. 9. (a) The logarithm of dc conductivity of the partially annealed (at 500°C for 10 h) $\text{Bi}_{4-n}\text{Pb}_n\text{Sr}_3\text{Ca}_3\text{Cu}_4\text{O}_x$ glass ceramics as a function of T^{-1} with $n=0.1$ (\square), 0.5 (\bullet), and 1.0 (\circ). (b) The logarithm of the low-temperature ($T < 125$ K) conductivity of the partially annealed at 500°C for 10 h) $\text{Bi}_{4-n}\text{Pb}_n\text{Sr}_3\text{Ca}_3\text{Cu}_4\text{O}_x$ [for Pb1A ($n=0.1$) (\times), Pb2A ($n=0.5$) (\circ), and Pb3A ($n=1.0$) (\bullet)] glass ceramics as a function of $T^{-1/4}$.

data plotted in Fig. 9(a). The Debye temperature θ_D , estimated from the temperature where nonlinearity begins, varies from 465 to 488 K with Pb concentration (Table IV) and these θ_D values for these partially annealed glasses are greater than those of the as-quenched glasses (Table I). These values of θ_D (465–488 K) also supports the theoretical value of the superconducting Bi-Pb-Sr-Ca-Cu-O system.^{30,31} But the Debye temperature shows opposite behaviors with increasing Pb concentration in as-quenched glasses (Table I) and in the partially annealed glass ceramics (Table IV), respectively. For the first case θ_D is decreasing with the increase of Pb concentration while for the second case it is increasing with increase of Pb content. Actually the procedure used in evaluating θ_D is not usual and quite rough. So this strange result might be due to the rough evaluation of θ_D in the partially annealed glass ceramics. Moreover, the multiple phases characterizing the annealed samples (observed from XRD pattern in Fig. 2) make the use of the appropriate techniques (ultrasounds and infrared spectroscopy) quite difficult for determining the correct values of θ_D . Therefore the corresponding values of θ_D must be considered only in the light of the order of magnitude. The characteristic phonon frequency $\nu_{\text{ph}} (=k_B \theta_D / h)$ also changes

TABLE IV. Values of different parameters of the annealed glass ceramics (the $\text{Bi}_{4-n}\text{Pb}_n\text{Sr}_3\text{Ca}_3\text{Cu}_4\text{O}_x$ glasses annealed at 500 °C for 10 h.

Parameters	Pb1A ($n=0.1$)	Pb2A ($n=0.5$)	Pb3A ($n=1.0$)
Density (gm/cc)	6.939	6.722	6.776
N (10^{21} cm^{-3})	9.63	9.39	9.49
R (Å)	4.704	4.739	4.723
r_p (Å)	1.88	1.91	1.90
θ_D (K)	465	476	488
ν_{ph} (10^{12} Hz)	9.70	993	10.18
$N(E_F)^a$	3.50	4.80	5.10
($10^{21} \text{ eV}^{-1} \text{ cm}^{-3}$)			
α (Å $^{-1}$)	0.018	0.019	0.019
W (eV) (at 300 K)	0.11	0.095	0.036
γ	5.49	4.68	1.71

with the increase of Pb as shown in Table IV (corresponding values for the as-quenched glasses as shown in Table I).

The dc conductivity of the partially annealed samples, viz. Pb1A, Pb2A, and Pb3A, in the low temperature region ($T < 125$ K) can be fitted with the equation²³

$$\sigma_{\text{dc}} = A \exp(-B/T^n). \quad (6)$$

The value of the exponent n determines the nature of the conduction mechanism in the semiconducting region of the sample. A and B in Eq. (6) are constants and

$$B = 2.1[\alpha^3/k_B N(E_F)]^{1/4}. \quad (7)$$

Experimental conductivity data are fitted with Eq. (6) using least squares method. The results are presented in Fig. 9(b). Below 125 K ($< \theta_D/2$), the resistivity of the samples may be well described by the relation (6) with $n = 1/4$. This suggests that the conduction in the low temperature region is governed by a three dimensional variable range hopping mechanism.²³

The $N(E_F)$ values of these partially annealed glass ceramics have been calculated from the corresponding ac conductivity measurement as in the case of as-quenched glasses. Table IV shows that these values of $N(E_F)$ lie between 10^{21} – $10^{22} \text{ eV}^{-1} \text{ cm}^{-3}$. These values of $N(E_F)$ of the partially annealed glass ceramics also agree quite well with those obtained from the superconducting Bi-2212 system.³

As mentioned above, the hopping conduction mechanism in all the partially annealed glasses changes to the adiabatic regime. From the plot of $\log_{10}(\sigma_{\text{dc}})$ vs W (Fig. 10), the estimated temperatures T_e (as in the case of as-quenched glass samples; Fig. 8) are 304 and 222 K which are very close to the corresponding experimental temperatures, viz. 300 and 220 K, respectively. This suggests²⁸ that the hopping mechanism is in the adiabatic regime. The Holstein condition²⁹ for adiabatic hopping [Eq. (5)] is also satisfied for these partially annealed glassy precursors. The values of α estimated from

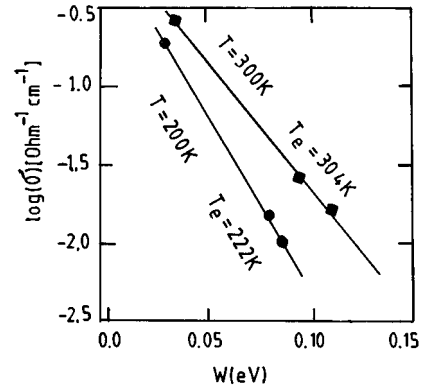


FIG. 10. The logarithm of the dc conductivity of the PbA-type samples as a function of W , at two fixed temperatures (at 220 and 300 K). The estimated temperatures from the slopes of these two curves are 222 and 304 K, respectively.

Eq. (7) using the values of $N(E_F)$ from Table IV are found to be very small and almost constant. These low values of α (Table IV) also support the adiabatic hopping mechanism. Therefore, a change over in hopping mechanism from non-adiabatic to adiabatic regime takes place when the as-quenched glasses are annealed at 500 °C for 10 h (similar behavior is also found for these glasses annealed at 300 °C for 24 h or more). Therefore, nonadiabatic hopping mechanism is true for the pure glassy precursors for high- T_c superconductors which is in contrast to the observation of Singh and Zacharias.¹⁴ The adiabatic hopping conduction is observed, due to the presence of more conducting microcrystals in these partially annealed glasses. It is important to mention here that these more conducting microcrystalline clusters might even form in the glass at the time of preparation which changes the conduction mechanism along with other properties.

Assuming the high temperature activation energy W to be close to the hopping energy W_H [Ref. 23], we can roughly estimate the electron-phonon coupling strength $\gamma = W_p/k_B \theta_D$, where W_p is the polaron binding energy and equal to $2W_H$. Activation energy W calculated from Fig. 9(a) (plot of $\ln \sigma$ vs $1000/T$) for a typical Pb1A sample, at room temperature, is about 0.11 eV. The electron-phonon coupling constant γ , calculated with this value of W , is 5.49. The values of γ decrease with increase of annealing time of the samples (Tables I and IV).

To get the idea about the size of polaron we use the formula²⁶ which has been used in the case of as-quenched glasses. For the Pb2A glass ceramic the radius of the polaron is estimated to be ~ 2 Å. We have also evaluated all these parameters for the as-quenched unannealed glasses (Table I). The values of r_p for the as-quenched and the partially annealed (at 500 °C for 10 h) glasses remain almost same (Tables I and IV). We have also tried to fit the dc conductivity data of the partially annealed PbA sample with the Schnakenberg model [Eq. (3)], but the fitting parameters obtained are not feasible.

Figure 11 shows the temperature dependences of the resistivity for the $\text{Bi}_{4-n}\text{Pb}_n\text{Sr}_3\text{Ca}_3\text{Cu}_4\text{O}_x$ ($n = 0.1, 0.5, 1.0$) glass ceramic (heat treated at 840 °C for 24 h). All these samples show metallic behavior above the superconducting transition temperature T_c , varying from 110 to 115 K. The

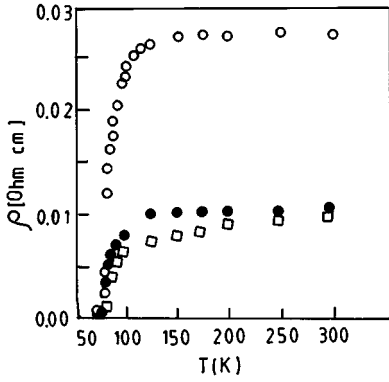


FIG. 11. Thermal variation of the resistivity of the superconducting $\text{Bi}_{4-n}\text{Pb}_n\text{Sr}_3\text{Ca}_3\text{Cu}_4\text{O}_x$ glass ceramics [with $n=0.1$ (Pb1S) (\square), 0.5 (Pb2S) (\bullet), and 1.0 (Pb3S) (\circ) annealed at 840°C for 24 h.

corresponding T_{c0} (zero resistance temperature) values are 72, 73, and 78 K, respectively, for $n=0.1$, 0.5 , and 1.0 .

D. Thermoelectric power

Thermoelectric power of all the Pb-doped as-quenched glassy semiconductors is found to be positive indicating holes are the carriers, which is due to donation of holes by the Pb ions. However, because of large resistances of the samples reliable TEP data of the glasses cannot be obtained. The thermal variation of TEP data of the partially annealed PBA glasses can be measured and are shown in Fig. 12. As observed from this figure, the TEP values increase with increase of temperature unlike many semiconducting oxide glasses where, as suggested by Heikes' model³² thermoelectric power $S = k/e[\ln(c/(1-c)) + a]$, where a is a constant, is almost temperature independent.

It is interesting to note that the temperature dependent TEP is drastically changed for the glass-ceramic superconductors (Fig. 13). Here, for all such samples, the temperature dependent TEP values are negative around 300 K and the sign changes from negative to positive around 290 K. As temperature decreases, the S increases exhibiting a peak around 115 K ($\sim T_c$) and then suddenly drops to zero at 72, 73, and 78 K (the zero resistance temperature, T_{c0}) for the Pb1S, Pb2S, and Pb3S samples, respectively. This behavior is consistent with the fact that in the superconducting state, the S becomes zero. The variation of S above 120 K of these samples is very similar to that obtained³³ for the doped La-Sr-Cu-O.

It has been suggested³⁴ that the Hubbard model well describes the basic physics of these high- T_c materials. For large on-site repulsion, the TEP for a Hubbard model (in the high temperature limit) is given by

$$S = -(k/|e|)\ln 2 - (k/|e|)\ln(p/1-p). \quad (8)$$

Entropy considerations lead to this formula with p equal to the ratio of Cu^{3+} to the Cu_t , if the conduction process involves hopping d electrons and/or holes from one Cu^{2+} to a Cu^{3+} ion. The $\ln 2$ term appears from the spin degree of freedom and would be absent if Cu^{2+} ions are magnetically

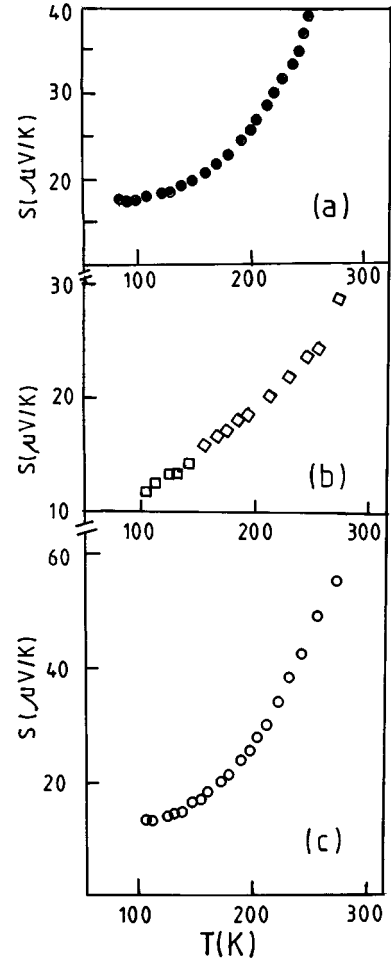


FIG. 12. Thermal variation of the thermoelectric power (S) of (a) Pb1A (\bullet), (b) Pb2A (\square), and (c) Pb3A (\circ).

ordered. On the other hand, if Cu^{2+} ions are not ordered and have twofold orbital degeneracy (which occurs for strictly octahedral symmetry) there would be an extra $\ln 2$ term from the orbital degrees of freedom. The magnetic ordering is absent in this system³⁵ and, therefore, the modified expression for TEP is

$$S = -(2k/|e|)\ln 2 - (2k/|e|)\ln(p/1-p). \quad (9)$$

At room temperature for our Pb1S superconducting sample, the hole concentration is 0.198 per Cu ion. For Pb2S and Pb3S the values of hole concentration are almost same (~ 0.199 per Cu ion). The values are slightly greater than the results obtained by Tarascon *et al.*³⁵ where, for the undoped $\text{Bi}_4\text{Sr}_3\text{Ca}_3\text{Cu}_4\text{O}_x$ (4334) ceramic superconductor, they found a hole concentration of 0.15 per Cu ion by TGA and titration experiments. This increase in hole concentration per Cu ion, in the present system, is simply due to doping of Pb as it acts as a hole donor.

We have also fitted the TEP data of our superconducting samples using the expression

$$S = [AT/(B^2 + T^2)] + \alpha'T, \quad (10)$$

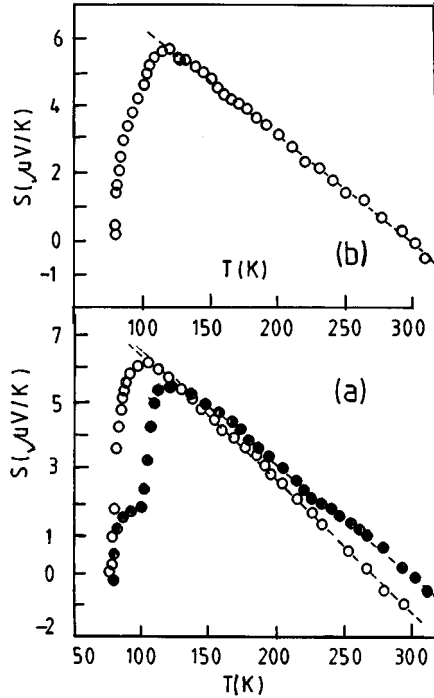


FIG. 13. The thermal variation of the thermoelectric power (S) of the superconducting $\text{Bi}_{4-n}\text{Pb}_n\text{Sr}_3\text{Ca}_3\text{Cu}_4\text{O}_x$ glass ceramics annealed at 840°C for 24 h: (a) $n=0.1$ (Pb1S) (\circ), $n=0.5$ (Pb2S) (\bullet), and (b) $n=1.0$ (Pb3S) (\circ). The dotted line represent the best fit curve with Eq. (10). The same best fit curve is obtained with Eq. (12).

which has been used by Forro *et al.*,³⁶ where the second term is the normal band contribution. The first term, as proposed by Gottwick *et al.*³⁷ for the analysis of the TEP data of CeNi_x samples, is obtained by assuming superposition of broad band and a localized band with a peak position at ϵ_0 and width Γ . The constants A and B are given by

$$A = 2(\epsilon_0 - \epsilon_F)/|e| \quad \text{and} \quad B^2 = [(\epsilon_0 - \epsilon_F)^2 + \Gamma^2]/\pi^2 k_B^2, \quad (11)$$

where ϵ_F is the Fermi energy. The TEP results of our samples fitted to Eq. (10) in the temperature range of 110–300 K are shown in Fig. 13. The best fit parameters A , B , and α' are given in Table V along with the values of $(\epsilon_0 - \epsilon_F)$ and Γ . For all the samples α' is found to be negative and nearly the same. However, with the increase of Pb concentration, $(\epsilon_0 - \epsilon_F)$ decreases but Γ increases systematically.

The TEP results of the glass ceramics which become superconductors after annealing at 840°C for 24 h have also been fitted with the Nagaosa-Lee model³⁸ which is actually a modification of the model proposed by Ikagawa *et al.*³⁹ Nagaosa and Lee proposed that for a superconducting cuprate, there are two contributions in the TEP, one coming from bosons (S_B) and another from fermions (S_F): $S = S_B + S_F$ with, $S_B = (k_B/e)[1 - \ln(2\pi p/mk_B T)]$ and $S_{qF} = -[k_B/e]k_B T/\epsilon_F$, where p is the concentration of holes per (Cu-O) bond and m is the mass of the bosonic carrier.

TABLE V. Best fit parameters A , B , and α' of Eq. (3) and F , G , and H of Eq. (4) and $(\epsilon_0 - \epsilon_F)$, Γ values determined from A and B of the superconducting glass ceramics obtained by annealing the $\text{Bi}_{4-n}\text{Pb}_n\text{Sr}_3\text{Ca}_3\text{Cu}_4\text{O}_x$ glasses at 840°C for 24 h.

Value of	Pb1S ($n=0.1$)	Pb2S ($n=0.5$)	Pb3S ($n=1.0$)
A (μV)	1880	1840	1800
B (K)	112	124	127
α' ($\mu\text{V}/\text{K}^2$)	-0.023	-0.018	-0.018
$(\epsilon_0 - \epsilon_F)$ (K)	10.9036	10.6716	10.4396
Γ (K)	202.853	224.658	230.116
F	0.0629	0.0637	0.0638
G (K)	5.95×10^7	5.95×10^7	6.00×10^7
H (K)	1.33×10^3	1.48×10^3	1.478×10^3

To fit the TEP results of some superconducting as well as nonsuperconducting compounds, Ikegawa *et al.* modified the above equation in the following form:

$$S = k_B/e[1 - F \ln(2\pi pG/T) - T/H], \quad (12)$$

where, F , G , and H are the fitting parameters.

The thermoelectric power of the superconducting samples can also be well fitted, like Eq. (10), to Eq. (12). The best fit curves obtained with Eqs. (10) and (12) are almost similar as shown in Fig. 13 [for the best fit with Eq. (10)]. The corresponding fitting parameters, viz. F , G , and H , are also shown in Table V.

IV. SUMMARY AND CONCLUSIONS

The $\text{Bi}_{4-n}\text{Pb}_n\text{Sr}_3\text{Ca}_3\text{Cu}_4\text{O}_x$ glass ceramics annealed at 500°C for 10 h remain semiconductor similar to the corresponding as-quenched glasses. Small polaron hopping conduction mechanism is valid for all these samples. However, a change over from the nonadiabatic small polaron hopping conduction mechanism to the adiabatic hopping conduction mechanism takes place with increase of annealing time and temperature (for instances at 500°C for 10 h and at 300°C for 24 h). This is due to the formation of microcrystals in these annealed glasses as observed from XRD patterns and SEM studies. It is important to note that such microcrystals might also form even in the as-quenched glasses (depending on quenching rate, etc.) and as a consequence such glasses would show the adiabatic hopping mechanism instead of the nonadiabatic hopping mechanism as observed by Singh and Zacharias¹⁴ and Som and Chaudhuri.¹⁷ It is further observed that the semiconducting behavior of the as-quenched and the partially annealed glasses, at low temperature, follow the variable range hopping conduction mechanism. The values of the density of states $N(E_F)$ also increase with annealing time. The thermal variation of thermoelectric power indicates that the Pb-doped Bi-Sr-Ca-Cu-O glasses and the corresponding glass ceramics are p -type semiconductors.

All the Pb-doped glasses of our present investigation become superconducting after annealing at 840°C for 24 h. The positive TEP values of these superconductors again indicate that the Pb-Bi-Sr-Ca-Cu-O type glass ceramics are

hole-type superconductors. It has also been found that the thermoelectric power of the superconducting glass ceramics varies systematically with the carrier concentrations (the carrier concentration is changed by substituting Pb at the Bi site). The zero value of the TEP at temperature T_{c0} is consistent with the corresponding zero resistance temperature of the glass-ceramic superconductor under investigation. The negative value of TEP around 300 K indicates the presence of both electrons and holes in the system. Similar coexistence of holes and electrons has also been very recently reported⁴⁰ in the superconducting $\text{BaBi}_{0.25}\text{Pb}_{0.75}\text{O}_{3-\delta}$ and $\text{Ba}_{0.74}\text{K}_{0.57}\text{BiO}_{3-\delta}$ oxides. Again since the Nagaosa-Lee model considers bosonic carriers and also fit the TEP data, the contribution of the bosons in the thermoelectric power appears to be important.

Finally, since the semiconducting behavior of the glassy and partially annealed Pb-doped system can be well explained by the small polaron hopping conduction mechanism, one might argue that the superconductivity in the

present glass ceramics (and in other related systems) is bipolaronic in origin.^{41,42} These bipolarons (or “spin polarons”⁴¹), might be created (with lowering of temperature) from the small polarons already existing in the glassy phase. Indeed, experimental evidence of polaron hopping has been reported in a layer structure of superconducting cuprates.⁴³

ACKNOWLEDGMENTS

The authors are grateful to the University Grants Commission (UGC), and to the Department of Science and Technology (DST) for providing financial assistance. The facilities for the XRD, SEM, EDX, IR, and atomic absorption studies provided by the Departments of Materials Science, Inorganic Chemistry, and Organic Chemistry are also gratefully acknowledged. The authors are also grateful to Professor H. Sakata of Tokai University, Japan, for his valuable comments.

- ¹Y. Abe, H. Hosono, M. Hosoe, J. Iwase, and Y. Kubo, *Appl. Phys. Lett.* **53**, 1341 (1988).
- ²S. Mollah, A. K. Chakraborty, S. Chakraborty, K. K. Som, and B. K. Chaudhuri, *J. Non-Cryst. Solids* **165**, 192 (1994).
- ³M. Onishi, M. Kyoto, and M. Watanwabe, *Jpn. J. Appl. Phys.* **30**, L1545 (1991).
- ⁴E. Takayama-Muromachi, Y. Uchida, A. Ono, F. Izumi, M. Onoda, Y. Matsui, K. Kasuda, S. Takekawa, and K. Kato, *Jpn. J. Appl. Phys.* **27**, 1365 (1988).
- ⁵E. Takayama-Muromachi, Y. Uchida, Y. Matsui, M. Onoda, and K. Kato, *Jpn. J. Appl. Phys.* **27**, L556 (1988).
- ⁶R. Ramesh, G. Thomas, S. M. Green, C. Jiang, Y. Mei, M. L. Rudee, H. L. Luo, and C. Politis, *Phys. Rev. B* **38**, 7070 (1988).
- ⁷M. Takano, J. Takada, K. Oda, H. Kitaguchi, Y. Miura, Y. Tomii, and H. Mazaki, *Jpn. J. Appl. Phys.* **27**, L1041 (1988).
- ⁸U. Endo, S. Koyama, and T. Kawai, *Jpn. J. Appl. Phys.* **28**, L190 (1989).
- ⁹T. Komatsu, R. Sato, K. Matusita, and T. Yamashita, *Appl. Phys. Lett.* **54**, 1169 (1989).
- ¹⁰L. R. Yuan, K. Kurosawa, Y. Takigawa, M. Okuda, H. Naito, K. Nakahigashi, S. Nakanishi, and T. Matsushita, *Jpn. J. Appl. Phys.* **30**, L1545 (1991).
- ¹¹R. C. Baker, W. M. Hurg, and H. Stienfink, *Appl. Phys. Lett.* **54**, 371 (1989).
- ¹²S. Mollah, K. K. Som, K. Bose, A. K. Chakraborty, and B. K. Chaudhuri, *Phys. Rev. B* **46**, 11 075 (1992).
- ¹³S. Mollah, K. K. Som, K. Bose, and B. K. Chaudhuri, *J. Appl. Phys.* **71**, 931 (1993).
- ¹⁴R. Sing and E. Zacharias (unpublished).
- ¹⁵S. Mollah, Ph.D. thesis, Jadavpur University, 1993.
- ¹⁶S. Mollah, S. Chatterjee, S. Chakraborty, and B. K. Chaudhuri, *Philos. Mag. B* **71**, 151 (1995).
- ¹⁷K. K. Som and B. K. Chaudhuri, *Phys. Rev. B* **41**, 1581 (1990).
- ¹⁸N. P. Bansal (unpublished).
- ¹⁹A. Poddar, P. Mandal, A. N. Das, B. Ghosh, and P. Choudhury, *Physica C* **161**, 567 (1989).
- ²⁰N. F. Mott, *J. Non-Cryst. Solids* **1**, 1 (1968).
- ²¹E. A. Davis and N. F. Mott, *Philos. Mag.* **22**, 903 (1970).
- ²²G. N. Greaves, *J. Non-Cryst. Solids* **11**, 427 (1973).
- ²³N. F. Mott, *Metal Insulator Transitions* (Taylor and Francis, London, 1974).
- ²⁴J. Schnakenberg, *Phys. Status Solidi* **28**, 623 (1968).
- ²⁵S. Mollah, K. K. Som, S. Chakraborty, A. K. Bera, S. Chatterjee, S. Banerjee, and B. K. Chaudhuri, *Phys. Rev. B* **51**, 17 512 (1995).
- ²⁶V. N. Bogomolov, E. K. Kudinov, and Yu. A. Firsov, *Sov. Phys. Solid State* **9**, 2502 (1968).
- ²⁷I. G. Austin and E. S. Garbett, in *Electronic and Structural Properties of Amorphous Semiconductors*, edited by P. G. Lecomber and J. Mort (Academic, London, 1973), p. 393.
- ²⁸M. Sayer and A. Mansingh, *Phys. Rev. B* **6**, 4629 (1972).
- ²⁹D. Emin and T. Holstein, *Ann. Phys. (N.Y.)* **21**, 439 (1963).
- ³⁰M. K. Yu, J. P. Frank, and S. Gyax, *Physica B* **165-166**, 1339 (1990).
- ³¹N. Okazaki, T. Hasegawa, K. Kishio, K. Kitazawa, A. Kishi, Y. Ikeda, M. Takano, K. Oda, H. Kitaguchi, J. Takada, and Y. Miura, *Phys. Rev. B* **41**, 4296 (1990).
- ³²R. R. Heikes and R. W. Ure, *Thermoelectricity* (Interscience, New York, 1961).
- ³³J. R. Cooper, B. Alavi, L. W. Zhou, W. P. Beyermann, and G. Grüner, *Phys. Rev. B* **35**, 8794 (1987).
- ³⁴P. W. Anderson, *Science* **235**, 1196 (1987).
- ³⁵J. M. Tarascon, Y. Le Page, P. Barboux, B. G. Bagles, L. H. Green, W. R. Mckinnon, G. W. Hull, M. Giroud, and D. M. Hwang, *Phys. Rev. B* **37**, 9382 (1988).
- ³⁶L. Forro, J. Lukatela, and B. Keszei, *Solid State Commun.* **73**, 501 (1990).
- ³⁷U. Gottwick, K. Gloos, S. Horn, F. Steglich, and N. Grewe, *J. Magn. Magn. Mater.* **47&48**, 536 (1985).
- ³⁸N. Nagaosa and P. A. Lee, *Phys. Rev. Lett.* **64**, 2450 (1990).
- ³⁹S. Ikagawa, T. Wada, T. Yamashita, A. Ichinose, K. Matsuura, K. Kubo, H. Ymanchi, and S. Tanaka, *Phys. Rev. B* **43**, 11 508 (1991).
- ⁴⁰T. Hashimoto and R. Hirasawa, T. Yoshida, Y. Yonemura, J. Mizusaki, and H. Tagawa, *Phys. Rev. B* **51**, 576 (1995). M. Rekala,

- R. Ratay, A. Pajazkauska, and B. Gegenheimer, *Phys. Status Solidi B* **155**, K123 (1989).
- ⁴¹N. F. Mott, *J. Condens. Matter* **5**, 3487 (1993).
- ⁴²A. S. Alexandrov and N. F. Mott, *Rep. Prog. Phys.* **57**, 1197 (1994); P. Prelovsek, T. M. Rice, and F. C. Zhang, *J. Phys. C* **20**, L229 (1987).
- ⁴³D. Mihailovic, C. M. Foster, K. Voss, and A. J. Heeger, *Phys. Rev. B* **42**, 7989 (1990); G. A. Samara, W. F. Hammett, and E. L. Venturini, *Phys. Rev. B* **41**, 8974 (1990).